

1      **Supplementary Information**

2

3      **The AAA+ chaperone VCP disaggregates Tau fibrils and generates**  
4                           **aggregate seeds**

5      Itika Saha<sup>1,2</sup>, Patricia Yuste-Checa<sup>1,2</sup>, Miguel Da Silva Padilha<sup>3,4</sup>, Qiang Guo<sup>5,#</sup>, Roman Körner<sup>1</sup>,  
6      Hauke Holthausen<sup>1</sup>, Victoria A. Trinkaus<sup>1,5,6</sup>, Irina Dudanova<sup>3,4</sup>, Rubén Fernández-  
7      Busnadio<sup>2,5,7,8</sup>, Wolfgang Baumeister<sup>5</sup>, David W. Sanders<sup>9,‡</sup>, Saurabh Gautam<sup>1,§</sup>,  
8      Marc I. Diamond<sup>9</sup>, F. Ulrich Hartl<sup>1,2,6,\*</sup> and Mark S. Hipp<sup>1,6,10,11\*</sup>

9

10     <sup>1</sup>Department of Cellular Biochemistry, Max Planck Institute of Biochemistry, Am Klopferspitz  
11     18, 82152 Martinsried, Germany.

12     <sup>2</sup>Aligning Science Across Parkinson's (ASAP) Collaborative Research Network, Chevy Chase,  
13     MD, USA.

14     <sup>3</sup>Molecular Neurodegeneration Group, Max Planck Institute of Neurobiology,  
15     82152 Martinsried, Germany.

16     <sup>4</sup>Department of Molecules – Signaling – Development, Max Planck Institute of Neurobiology,  
17     Am Klopferspitz 18, 82152 Martinsried, Germany.

18     <sup>5</sup>Department of Structural Molecular Biology, Max Planck Institute of Biochemistry, Am  
19     Klopferspitz 18, 82152 Martinsried, Germany.

20     <sup>6</sup>Munich Cluster for Systems Neurology (SyNergy), Munich, Germany.

21     <sup>7</sup>Institute of Neuropathology, University Medical Center Göttingen, 37099 Göttingen, Germany.

22     <sup>8</sup>Cluster of Excellence “Multiscale Bioimaging: from Molecular Machines to Networks of  
23     Excitable Cells” (MBExC), University of Göttingen, Germany.

24     <sup>9</sup>Center for Alzheimer's and Neurodegenerative Diseases, Peter O'Donnell Jr. Brain Institute,  
25     University of Texas Southwestern Medical Center, Dallas, 75390 Texas, USA.

26     <sup>10</sup>School of Medicine and Health Sciences, Carl von Ossietzky University Oldenburg,  
27     Oldenburg, Germany.

28     <sup>11</sup>Department of Biomedical Sciences of Cells and Systems, University Medical Center  
29     Groningen, University of Groningen, Antonius Deusinglaan, 1, 9713 AV Groningen, The  
30     Netherlands.

31     # Present address: State Key Laboratory of Protein and Plant Gene Research, School of Life  
32     Sciences and Peking-Tsinghua Center for Life Sciences, Peking University, Beijing 100871,  
33     China.

34 ‡ Present address: Department of Chemical and Biological Engineering, Princeton University,  
35 Princeton, NJ 08544, USA

36 § Present address: Boehringer Ingelheim International GmbH, 55216 Ingelheim, Germany and  
37 ViraTherapeutics GmbH, 6063 Rum, Austria.

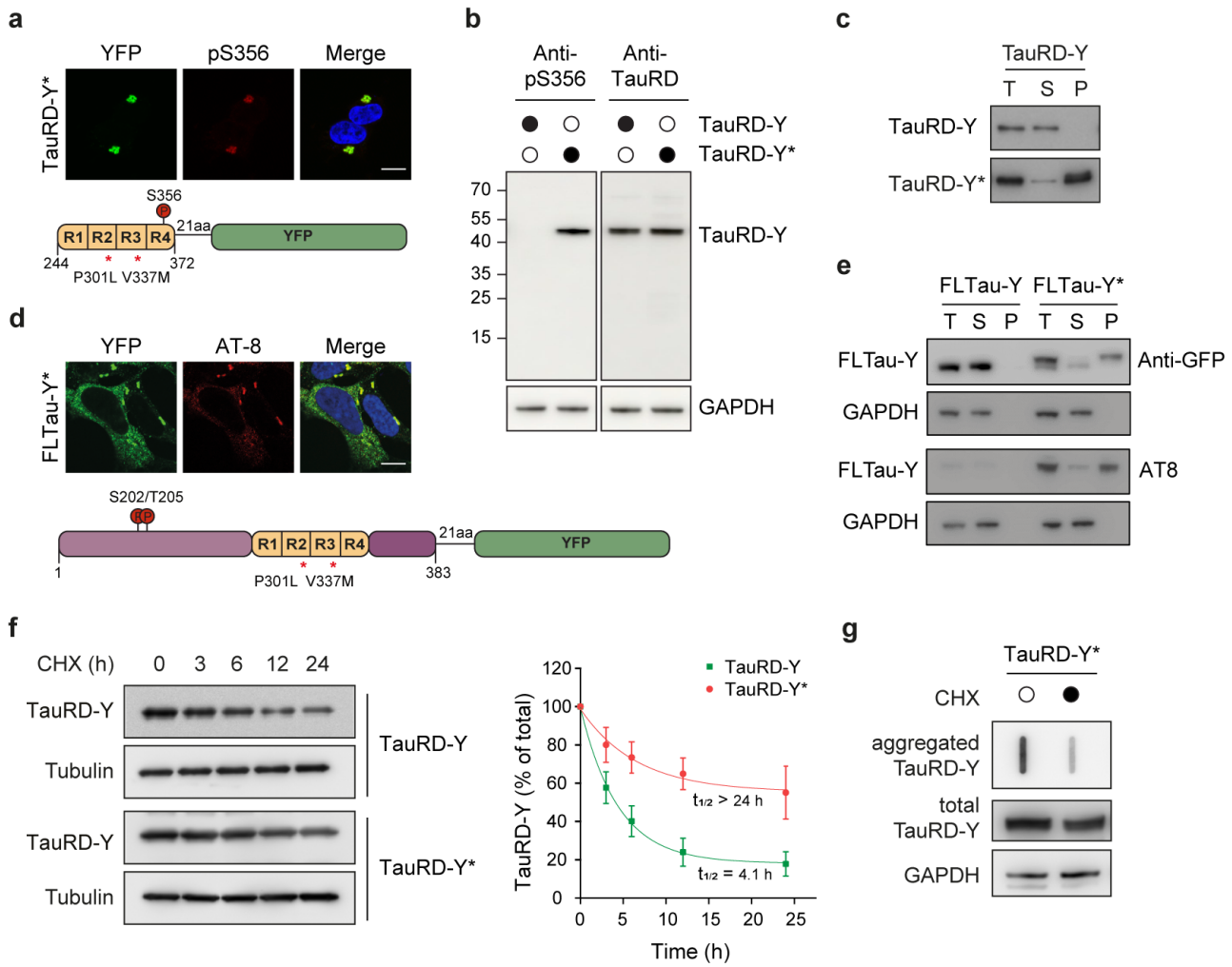
38

39 \*Correspondence to [uhartl@biochem.mpg.de](mailto:uhartl@biochem.mpg.de) and [m.s.hipp@umcg.nl](mailto:m.s.hipp@umcg.nl)

40

41 Supplementary information includes 10 Supplementary Figures and 1 Table

42

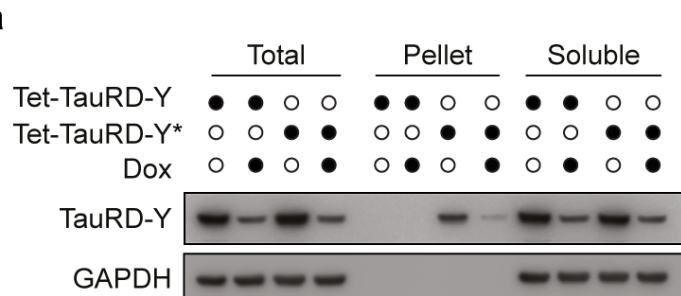


43

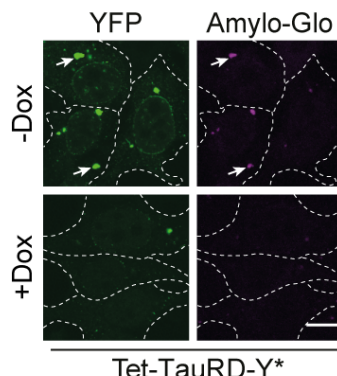
44 **Supplementary Fig. 1: Tau aggregation and clearance in a constitutive expression model.**

45 **a** Immunofluorescence staining of TauRD-Y\* cells with an antibody against Tau  
46 phosphorylation at S356 (red) and YFP fluorescence of TauRD-Y (green). Scale bar, 10  $\mu$ m.  
47 **b** Analysis of Tau S356 phosphorylation in lysates of TauRD-Y and TauRD-Y\* cells by  
48 immunoblotting. Total TauRD-Y was detected using antibody against TauRD. **c** Solubility of  
49 TauRD-Y in TauRD-Y and TauRD-Y\* cells at steady state, determined by fractionation of cell  
50 lysate by centrifugation, followed by immunoblotting with anti-GFP antibody. T, total cell  
51 lysate, S, supernatant, P, pellet. **d** Immunofluorescence staining of full-length Tau (FLTau-Y) in  
52 aggregate-containing FLTau-Y\* cells with AT-8 antibody specific for Tau phosphorylation at  
53 S202/T205 (red) and YFP fluorescence of TauRD-Y (green). Scale bar, 10  $\mu$ m. **e** Solubility of  
54 phosphorylated FLTau-Y in FLTau-Y and FLTau-Y\* cells at steady state analyzed as in (c).  
55 Immunoblotting was with AT-8 antibody (bottom) and anti-GFP (top). GAPDH served as  
56 loading control. **f** Turnover of TauRD-Y in TauRD-Y and TauRD-Y\* cells upon cycloheximide  
57 (CHX) shut-off (CHX; 50  $\mu$ g/mL). Left, anti-GFP immunoblots to determine TauRD-Y levels.  
58 Tubulin served as loading control. Right, exponential fits of CHX chase data and corresponding  
59 half-lives ( $t_{1/2}$ ). Mean  $\pm$  s.d.; n=3. **g** Filter trap analysis of aggregated TauRD-Y upon CHX chase  
60 for 24 h. Aggregated and total TauRD-Y levels were determined by anti-GFP immunoblotting.  
61 GAPDH served as loading control.

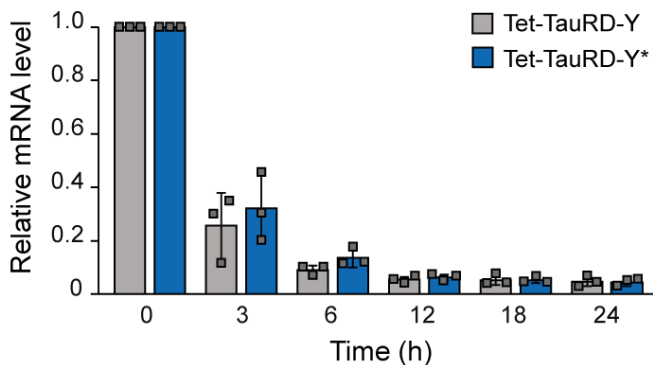
62



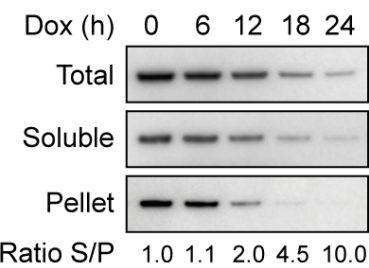
63



64



65



66

#### Supplementary Fig. 2: TauRD-Y aggregation and clearance upon inhibition of expression in a Tet-regulated TauRD-Y expression system.

**a** Solubility of TauRD-Y in Tet-TauRD-Y and Tet-TauRD-Y\* cells upon addition of 50 ng/mL doxycycline (Dox) for 24 h. Cell lysates were fractionated as in Supplementary Fig. 1c. TauRD-Y was detected with anti-GFP antibody. GAPDH served as loading control. **b** Representative fluorescence images of Tet-TauRD-Y\* cells treated with Dox for 24 h showing staining of TauRD-Y inclusions (green) with Amylo-Glo (magenta). White dashed lines indicate cell boundaries. Scale bar, 10  $\mu$ m. **c** Quantitative PCR analysis of TauRD-Y mRNA in Tet-TauRD-Y and Tet-TauRD-Y\* cells treated with Dox for 0, 3, 6, 12, 18 and 24 h. mRNA levels were normalized to the reference gene *RPS18*. Mean  $\pm$  s.d.; n=3. **d** Solubility of TauRD-Y in Tet-TauRD-Y\* cells upon addition of Dox for the indicated times. Normalized ratios of TauRD-Y in soluble (S) and pellet (P) fractions are stated.

67

68

69

70

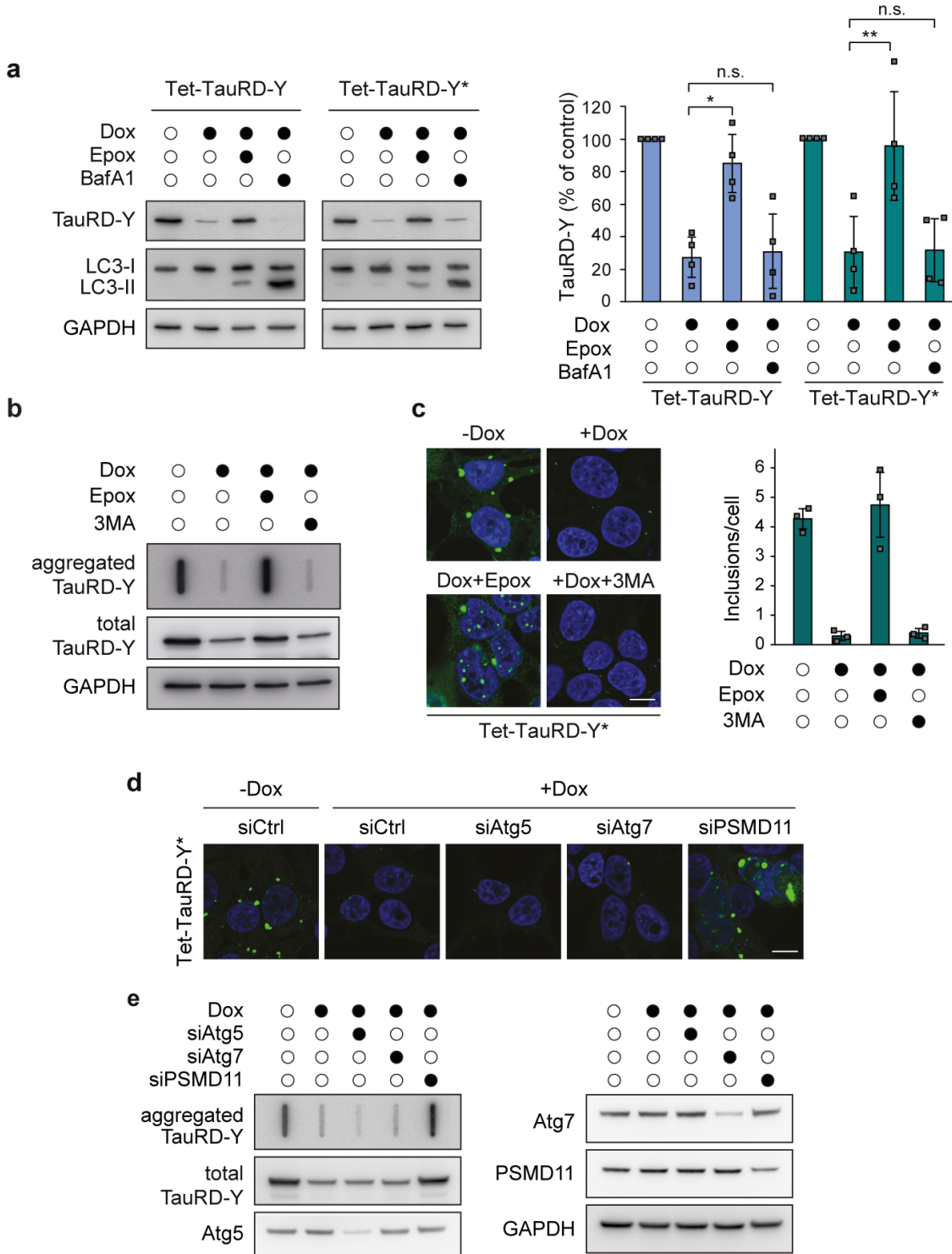
71

72

73

74

75

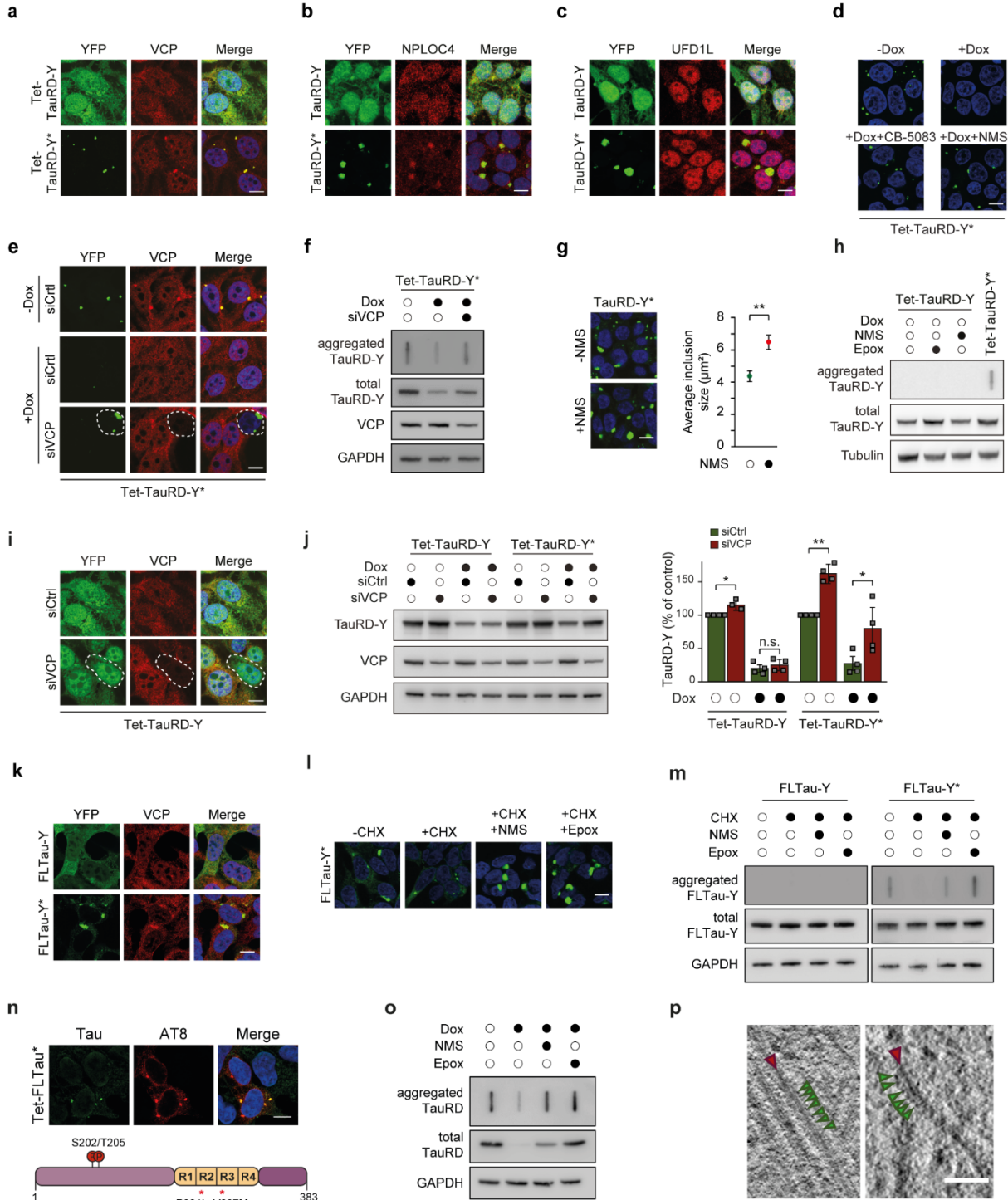


76  
77

78 **Supplementary Fig. 3: Effect of UPS and autophagy inhibition on TauRD-Y levels and**  
79 **aggregate clearance.**

80 **a** Analysis of TauRD-Y levels in Tet-TauRD-Y and Tet-TauRD-Y\* cells treated for 24 h with  
81 doxycycline (Dox; 50 ng/mL) alone or in combination with Epoxomicin (Epox; 50 nM) or

82 Bafilomycin A1 (BafA1; 50 nM). TauRD-Y and LC3 levels were determined by immunoblotting  
83 against GFP and LC3B respectively. GAPDH served as loading control. Mean  $\pm$  s.d.; n=4.  
84 \* $p<0.05$  (Tet-TauRD-Y: + Dox vs + Dox + Epox,  $p=0.0114$ ), \*\* $p<0.01$  (Tet-TauRD-Y\*: + Dox  
85 vs + Dox + Epox,  $p=0.0026$ ); n.s. non-significant (Tet-TauRD-Y: + Dox vs + Dox + Epox,  $p=$   
86 0.6422; Tet-TauRD-Y\*: + Dox vs + Dox + Epox,  $p=0.8799$ ) from two-tailed Student's paired t-  
87 test. **b** Filter trap analysis of Tet-TauRD-Y\* cells treated for 24 h with Dox alone or in  
88 combination with Epoxomicin (Epox; 50 nM) or 3-methyladenine (3MA; 5 mM). Aggregated  
89 and total TauRD-Y was detected with anti-GFP antibody. **c** Left, representative images of Tet-  
90 TauRD-Y\* cells treated for 24 h with Dox alone or, in combination with Epoxomicin (Epox;  
91 50 nM) or 3MA (5 mM). Scale bar, 10  $\mu$ m. Right, quantification of TauRD-Y foci. 100-200 cells  
92 analyzed per experiment. Mean  $\pm$  s.d.; n=3. **d** Representative images of Tet-TauRD-Y\* cells  
93 transfected with non-targeted (Ctrl) siRNA or siRNA against Atg5 (50 nM), Atg7 (50 nM) and  
94 PSMD11 (25 nM). 72 h after transfection, doxycycline (Dox; 50 ng/mL) was added for another  
95 24 h where indicated. Scale bar, 10  $\mu$ m. **e** Filter trap analysis of Tet-TauRD-Y\* cells transfected  
96 with siRNAs and treated with Dox as stated in (d). TauRD-Y was detected by immunoblotting  
97 with anti-GFP antibody.

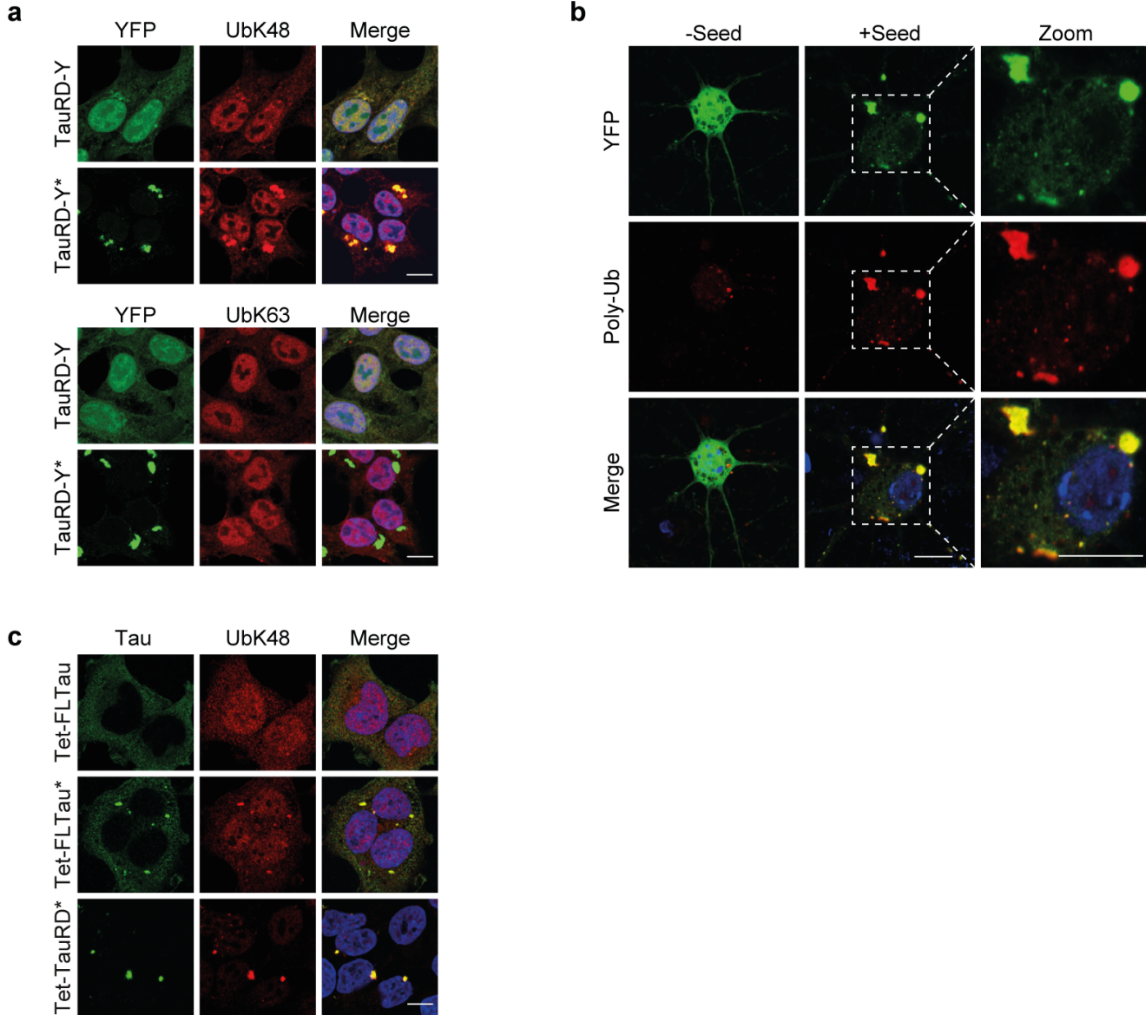


98

#### 99 Supplementary Fig. 4: Aggregation specific stabilization of Tau by VCP inactivation.

100 **a** Immunofluorescence staining of VCP (red) and YFP fluorescence of TauRD-Y (green) in Tet-  
101 TauRD-Y and Tet-TauRD-Y\* cells. **b** and **c** Immunofluorescence staining of NPLOC4 (b) (red)  
102 and UFD1L (c) (red) in TauRD-Y and TauRD-Y\* cells. Scale bars, 10  $\mu\text{m}$ . **d** Representative  
103 images of Tet-TauRD-Y\* cells treated for 24 h with doxycycline (Dox; 50 ng/mL) alone or in

104 combination with CB-5083 (1  $\mu$ M) or NMS-873 (NMS; 2.5  $\mu$ M). Scale bar, 10  $\mu$ m.  
105 **e** Immunofluorescence staining of VCP (red) in Tet-TauRD-Y\* cells treated with non-targeted  
106 (Ctrl) or VCP siRNA for 96 h. Doxycycline (Dox; 50 ng/mL) was added for the last 24 h.  
107 Dashed lines indicate a cell with reduced VCP levels. Scale bar, 10  $\mu$ m. **f** Filter trap analysis of  
108 aggregated TauRD-Y in Tet-TauRD-Y\* lysates treated as in (d). Aggregated and total TauRD-Y  
109 was analyzed by anti-GFP immunoblotting. GAPDH served as loading control. **g** Size increase  
110 of TauRD-Y inclusions upon VCP inhibition. Representative images of TauRD-Y\* cells treated  
111 for 24 h with NMS-873 (NMS; 5  $\mu$ M) and quantification of average inclusion size ( $\mu$ m<sup>2</sup>). 200-  
112 400 cells analyzed per experiment. Mean  $\pm$  s.d.; n=5. \*\*p<0.01 (p= 0.0022) from two-tailed  
113 Student's paired t-test. **h** Filter trap analysis of Tet-TauRD-Y cells treated for 24 h with  
114 Epoxomicin (Epox; 50 nM) or NMS-873 (NMS; 2.5  $\mu$ M) where indicated. Tet-TauRD-Y\* lysate  
115 was used as control. TauRD-Y was detected by immunoblotting with anti-GFP antibody.  
116 **i** Immunofluorescence staining of VCP (red) and YFP fluorescence of TauRD-Y (green) in Tet-  
117 TauRD-Y cells transfected with non-targeted (Ctrl) or VCP siRNA for 96 h. Dashed lines  
118 indicate a cell with reduced VCP levels. Scale bar, 10  $\mu$ m. **j** Left, analysis of TauRD-Y level in  
119 Tet-TauRD-Y and Tet-TauRD-Y\* cells transfected for 96 h with non-targeted (Ctrl) or VCP  
120 siRNA where indicated. Doxycycline (Dox; 50 ng/mL) was added for the last 24 h. TauRD-Y  
121 was detected by immunoblotting with anti-GFP antibody. Right, quantification of TauRD-Y  
122 immunoblot. Mean  $\pm$  s.d.; n=4. \*p<0.05 (Tet-TauRD-Y - Dox: siCtrl vs siVCP, p= 0.0218; Tet-  
123 TauRD-Y\* + Dox: siCtrl vs siVCP, p= 0.0156); \*\*p<0.01 (Tet-TauRD-Y\* - Dox: siCtrl vs  
124 siVCP, p= 0.0023); n.s. non-significant (Tet-TauRD-Y + Dox: siCtrl vs siVCP, p= 0.0539) from  
125 two-tailed paired Student's t-test. **k** Immunofluorescence staining of VCP (red) and YFP  
126 fluorescence of FLTau-Y (green) in FLTau-Y and FLTau-Y\* cells. Scale bar, 10  $\mu$ m.  
127 **l** Representative images of FLTau-Y\* cells treated for 24 h with cycloheximide (CHX; 50  
128  $\mu$ g/mL) alone or in combination with NMS-873 (NMS; 2.5  $\mu$ M) or Epoxomicin (Epox; 100 nM).  
129 Scale bar, 10  $\mu$ m. **m** Filter trap analysis of lysates from FLTau-Y and FLTau-Y\* cells treated for  
130 24 h with Dox alone or in combination with NMS-873 (NMS; 2.5  $\mu$ M) or Epoxomicin (Epox;  
131 50 nM). Aggregated and total FLTau-Y levels were determined by immunoblotting against GFP.  
132 GAPDH served as loading control. **n** Immunofluorescence staining of full-length Tau (FLTau) in  
133 aggregate-containing Tet-FLTau\* cells with Tau (green) and Tau S202/T205 phosphorylation  
134 specific AT-8 (red) antibody. Scale bar, 10  $\mu$ m. **o** Filter trap analysis of lysates from Tet-  
135 TauRD\* cells treated for 24 h with Dox alone or in combination with NMS-873 (NMS; 2.5  $\mu$ M)  
136 or Epoxomicin (Epox; 50 nM). Aggregated and total TauRD levels were determined by  
137 immunoblotting against myc and TauRD, respectively. GAPDH served as loading control.  
138 **p** Examples of two TauRD-Y fibrils from a representative 1.4 nm thick tomographic slice of a  
139 TauRD inclusion from neurons. Red arrows indicate TauRD-Y fibrils and green arrows indicate  
140 globular densities along fibrils. Scale bar, 40 nm.

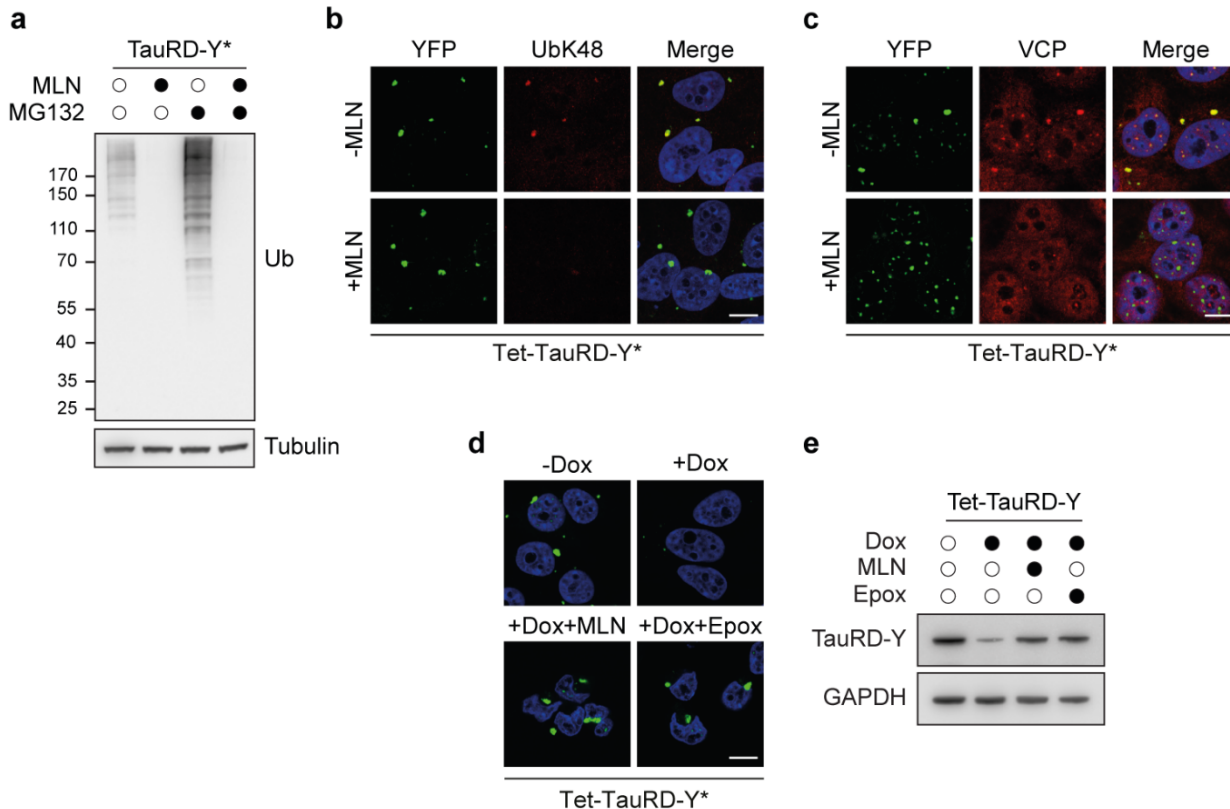


142

143 **Supplementary Fig. 5: Ubiquitylation of TauRD-Y aggregates.**

144 **a** Immunofluorescence staining of (top) ubiquitin-K48 (UbK48) (red) and (bottom) ubiquitin  
145 K63 (UbK63) (red) chains and YFP fluorescence of TauRD-Y (green) in TauRD-Y and TauRD-  
146 Y\* cells. Scale bars, 10  $\mu$ m. **b** Immunofluorescence staining of ubiquitylated proteins (FK2  
147 antibody) (red) in primary neurons expressing TauRD-Y (green) and treated with TauRD  
148 containing lysates (+Seed) where indicated. Scale bars, 20  $\mu$ m. **c** Immunofluorescence staining  
149 of ubiquitin-K48 (UbK48) (red) chains and Tau (green) in Tet-FLTau, Tet-FLTau\* and Tet-  
150 TauRD\* cells. FLTau was detected using Tau-5 and TauRD using anti-myc antibody. Scale bar,  
151 10  $\mu$ m.

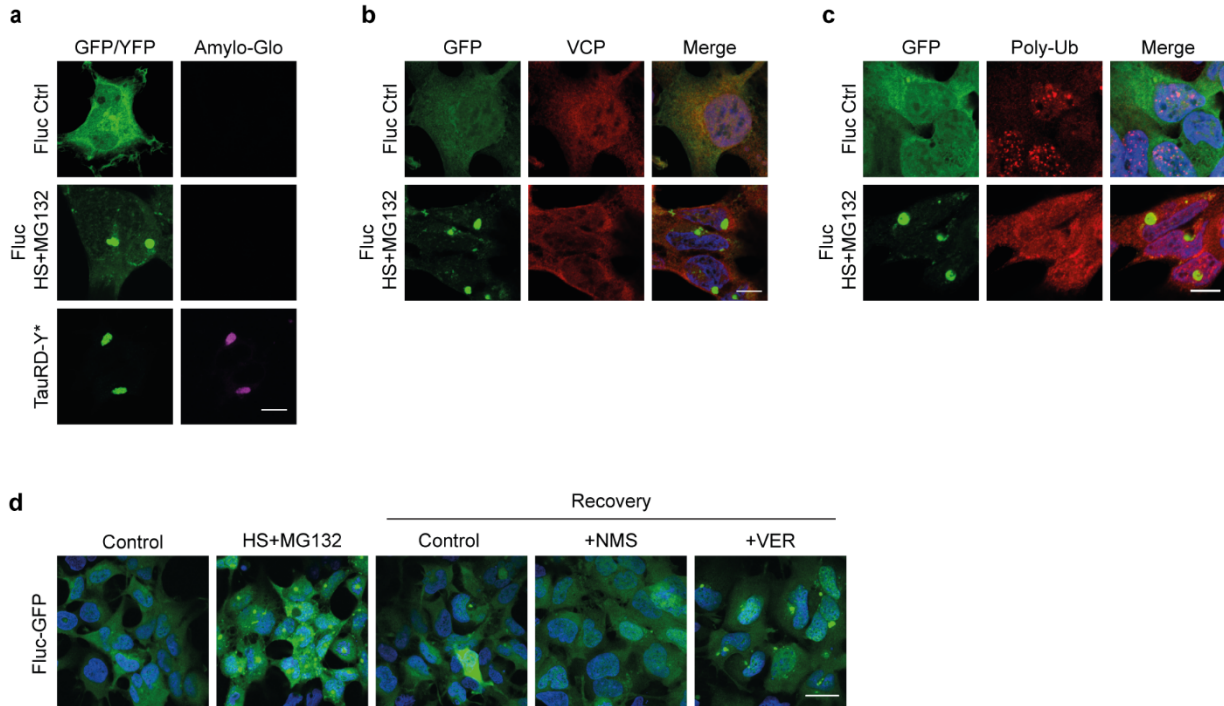
152



153

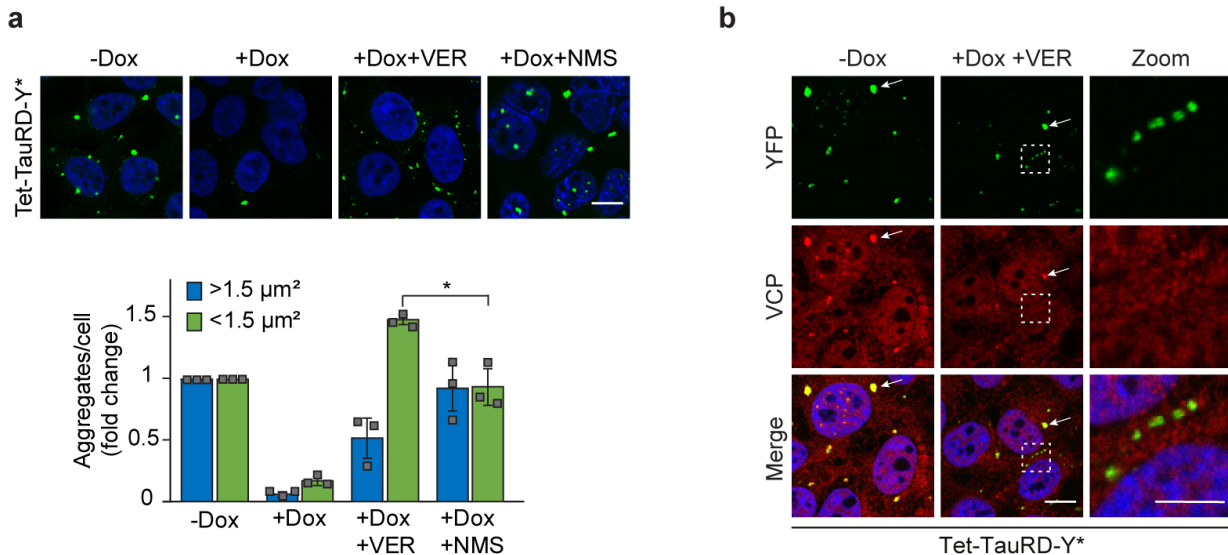
154 **Supplementary Fig. 6: Role of ubiquitylation in TauRD-Y disaggregation.**

155 **a** Analysis of ubiquitylated protein levels in lysates of TauRD-Y\* cells treated with the ubiquitin  
 156 activating enzyme E1 inhibitor MLN7243 (MLN; 0.5  $\mu$ M) alone or in combination with  
 157 proteasome inhibitor MG132 (1  $\mu$ M) for 14 h. Ubiquitylated proteins were detected by  
 158 immunoblotting against ubiquitin. Tubulin served as loading control. **b** Immunofluorescence  
 159 staining of ubiquitin-K48 chains (UbK48) (red) and **c** VCP (red) in Tet-TauRD-Y\* cells treated  
 160 with MLN7243 (MLN; 0.5  $\mu$ M) for 12 h. Scale bars, 10  $\mu$ m. **d** Representative images of Tet-  
 161 TauRD-Y\* cells treated for 24 h with doxycycline (Dox; 50 ng/mL) alone or in combination  
 162 with MLN7243 (MLN; 0.5  $\mu$ M) or Epoxomicin (Epox; 50 nM). Scale bar, 10  $\mu$ m. **e** Analysis of  
 163 TauRD-Y levels in Tet-TauRD-Y cells treated for 24 h with Dox, MLN7243 and Epoxomicin as  
 164 in (d). GAPDH served as loading control.  
 165



166

167 **Supplementary Fig. 7: Effect of VCP inhibition on firefly luciferase (Fluc) disaggregation.**  
168 **a** Fluc-GFP expressing cells maintained at 37 °C (Fluc Ctrl) or heat-stressed at 43 °C in presence  
169 of 5 μM MG132 for 2 h (Fluc HS) were stained with the amyloid-specific dye Amylo-Glo  
170 (magenta). TauRD-Y\* cells were used as control. Amylo-Glo fluorescence was imaged with  
171 similar exposure settings in all panels. Scale bar, 10 μm. **b** Immunofluorescence staining of VCP  
172 (red), and **c** ubiquitylated proteins (FK2 antibody) (red) in Fluc-GFP cells treated as in (a). Scale  
173 bars, 10 μm. **d** Effect of VCP and Hsp70 inhibition on Fluc-GFP disaggregation. Fluc-GFP  
174 aggregation was induced as in (a). Cells were then shifted to MG132 free media and allowed to  
175 recover at 37 °C for 8 h in presence of NMS-873 (NMS; 2.5 μM) and VER-155008 (VER; 10  
176 μM) where indicated. Scale bar, 30 μm.

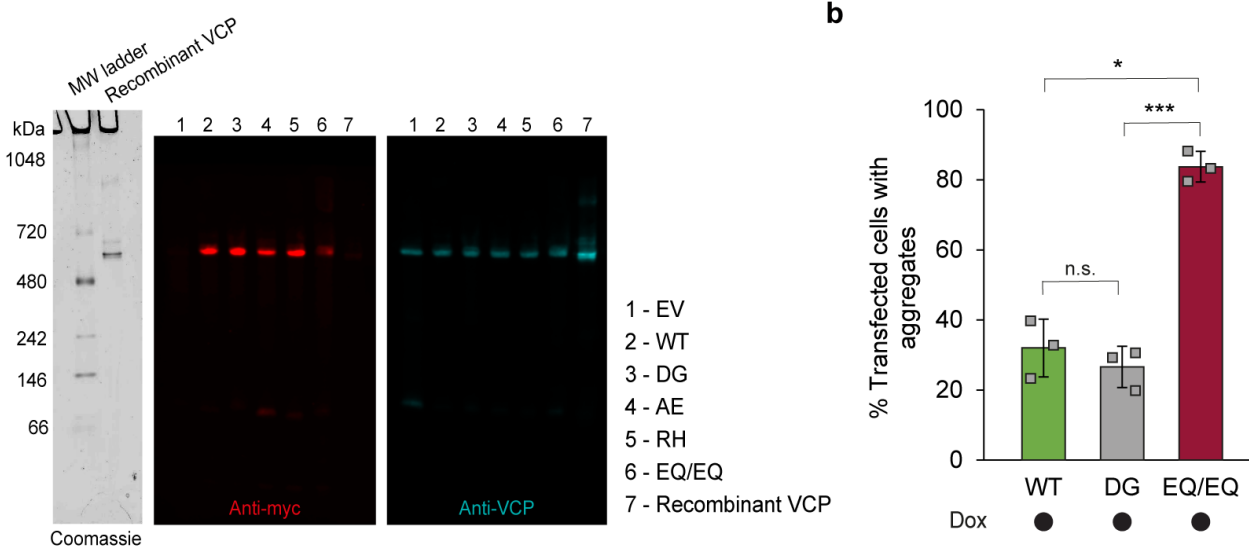


177

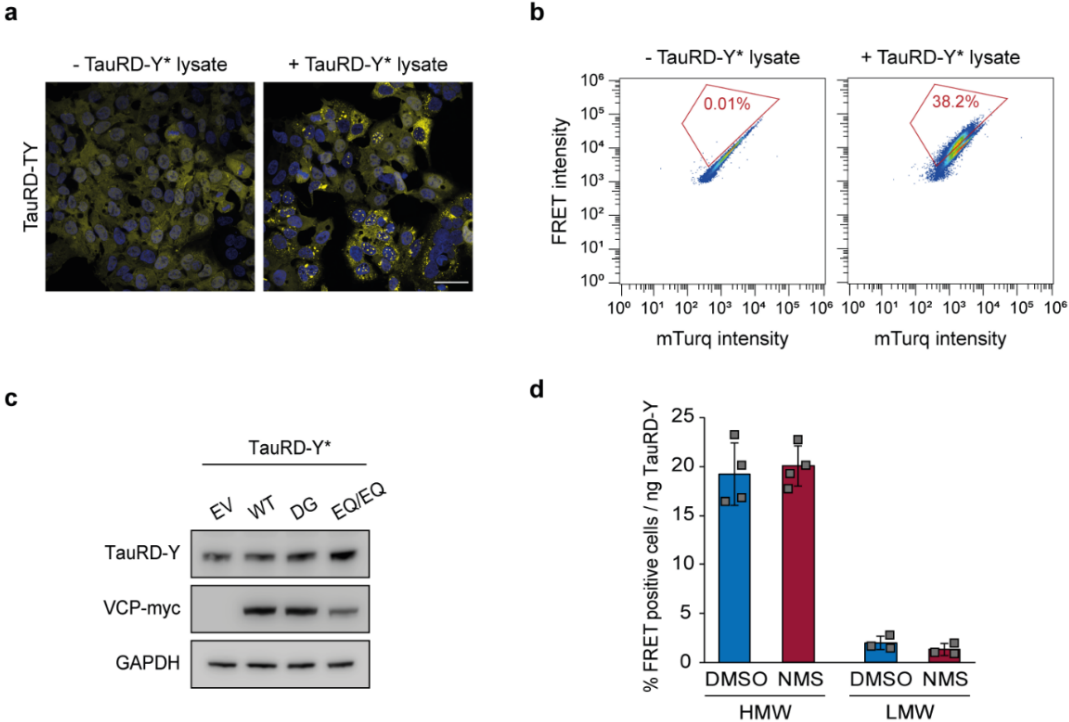
178 **Supplementary Fig. 8: Role of Hsp70 in TauRD-Y disaggregation.**

179 **a** Top, Representative images of Tet-TauRD-Y\* cells treated for 24 h with doxycycline (Dox; 50  
180 ng/mL) alone or in combination with VER-155008 (VER; 10  $\mu\text{M}$ ) or NMS-873 (NMS; 2.5  $\mu\text{M}$ ).  
181 Bottom, quantification of large ( $>1.5 \mu\text{m}^2$ ) and small ( $<1.5 \mu\text{m}^2$ ) TauRD-Y foci. Mean  $\pm$  s.d.;  
182 n=3; ~100-200 cells were analyzed per experiment. \*p<0.05 (p=0.0435) from two-tailed  
183 Student's paired t-test. Scale bar, 10  $\mu\text{m}$ . **b** Immunofluorescence staining of VCP (red) and YFP  
184 fluorescence of TauRD-Y (green) in Tet-TauRD-Y\* cells treated with a combination of  
185 doxycycline (Dox) and VER-155008 (VER) where indicated. White arrow points to large  
186 TauRD-Y inclusions co-localizing with VCP. Dashed lines enclose TauRD-Y foci that do not co-  
187 localize with VCP. Scale bar, 10  $\mu\text{m}$ . Scale bar zoom, 5  $\mu\text{m}$ .

188

189  
190

191     **a** Native-PAGE analysis of recombinant VCP and lysates from Tet-TauRD-Y\* cells transfected  
 192     with empty vector (EV) and myc-tagged wild type (WT), D395G (DG), A232E (AE), R155H  
 193     (DG) and E305Q/E578Q (EQ/EQ) VCP constructs. Immunoblot probed against myc (red) and  
 194     VCP (cyan) is shown. Non-tagged, recombinant VCP was analyzed as control. **b** Quantification  
 195     of aggregate foci in myc-positive Tet-TauRD-Y\* cells transfected with myc-tagged WT, DG and  
 196     EQ/EQ VCP constructs for 24 h, and treated for another 24 h with doxycycline (Dox; 50 ng/mL).  
 197     Mean  $\pm$  s.d.; n=3; > 100 cells analyzed per experiment; \*p<0.05 (WT vs EQ/EQ p=0.0192);  
 198     \*\*\*p<0.001 (DG vs EQ/EQ p=0.0008); n.s. non-significant (p=0.5646).  
 199



200

201 **Supplementary Fig. 10: Analysis of seeding-competent TauRD-Y.**

202 **a** Representative images of TauRD-TY FRET reporter cells treated with TauRD-Y\* lysate where  
 203 indicated showing TauRD-Y fluorescence in yellow. Scale bar, 40  $\mu$ m. **b** Representative  
 204 pseudocolour dot plots for the analysis of FRET positive TauRD-TY cells by flow cytometry  
 205 upon addition of TauRD-Y\* lysate. FRET intensity is plotted against mTurquoise2 (mTurq)  
 206 intensity and the % of FRET positive cells are indicated in red gates. **c** Analysis of TauRD-Y and  
 207 VCP-myc levels in TauRD-Y\* cells transfected for two days with empty vector (EV) and myc-  
 208 tagged wild type (WT), D395G (DG) and E305Q/E578Q (EQ/EQ) VCP constructs. TauRD-Y  
 209 and overexpressed VCP levels were determined by immunoblotting against GFP and myc,  
 210 respectively. GAPDH served as loading control. **d** Comparison of seeding efficiencies of high  
 211 molecular weight (HMW) and low molecular weight (LMW) species obtained by size exclusion  
 212 chromatography of lysates from TauRD-Y\* cells treated for 24 h with DMSO or NMS-873  
 213 (NMS; 2  $\mu$ M). Mean  $\pm$  s.d.; HMW n=4, LMW n=3.





P60228;E5RGA	Eukaryotic translation initiation factor EIF3E	sp P60228 EIF3E_HUMAN Eukaryotic translation initiation fac	25	52,22	2,3804	2,2127	1,9171	2,2127	1089300	1573400	1367200
P49916;K7ERZ!	DNA ligase 3 LIG3	sp P49916 DNL13_HUMAN DNA ligase 3 OS=Homo sapiens OX=946440	8	112,91	2,9178	2,203	2,1767	2,203	1532800	1039000	946440
Q5RKV6	Exosome complex component MTR3 EXOSC6	sp Q5RKV6 EXOSC6_HUMAN Exosome complex component MTI	6	28,235	2,3573	2,1818	2,111	2,1818	11071000	15292000	4620400
P12931	Proto-oncogene tyrosine-protein kinase SRC	sp P12931 SRC_HUMAN Proto-oncogene tyrosine-protein kinase SRC	8	59,834	2,168	4,1415	1,8886	2,168	748320	2601200	1702500
P63092;Q5JWF	Guanine nucleotide-binding protein G( GNAS	sp P63092 GNAS2_HUMAN Guanine nucleotide-binding protein G( GNAS	13	45,664	2,1627	4,1417	1,5402	2,1627	1488700	9048500	3740200
O75531;E9PJ8	Barrier-to-autointegration factor;Barrie BANF1	sp O75531 BAF_HUMAN Barrier-to-autointegration factor OS=Homo sapiens OX=175040000	6	10,058	2,1605	2,4895	1,4442	2,1605	167700000	464450000	175040000
Q9Y265;E7ETRC	RuvB-like 1 RUVBL1	sp Q9Y265 RUVBL1_HUMAN RuvB-like 1 OS=Homo sapiens OX=382330	24	50,227	1,8486	2,1597	2,5745	2,1597	2800700	6342500	382330
O14578;H7BYJ	Citron Rho-interacting kinase CIT	sp O14578 CTRO_HUMAN Citron Rho-interacting kinase OS=Homo sapiens OX=49921	11	231,43	3,1776	2,1397	0,96079	2,1397	57864	292140	49921
P27986;HOYBC	Phosphatidylinositol 3-kinase regulator PIK3R1	sp P27986 PIK3R1_HUMAN Phosphatidylinositol 3-kinase regulator PIK3R1	6	83,597	1,5657	2,1169	2,5085	2,1169	745890	1116000	1210500
Q6WCQ1;J3KS7	Myosin phosphatase Rho-interacting protein MPRIP	sp Q6WCQ1 MPRIP_HUMAN Myosin phosphatase Rho-interacting protein MPRIP	12	116,53	2,1049	2,173	0,79734	2,1049	588250	1624600	104110
P08754	Guanine nucleotide-binding protein G( GNAI3	sp P08754 GNAI3_HUMAN Guanine nucleotide-binding protein G( GNAI3	15	40,532	2,0157	4,9059	2,0813	2,0813	19273000	75469000	42160000
O15234;J3KS7	Protein CASC3 CASC3	sp O15234 CASC3_HUMAN Protein CASC3 OS=Homo sapiens OX=4126900	8	76,277	2,067	2,0138	2,7423	2,067	698630	2073400	4126900
P17987;E7EQRI	T-complex protein 1 subunit alpha TCP1	sp P17987 TCPA_HUMAN T-complex protein 1 subunit alpha C	34	60,343	1,5294	2,2873	2,0582	2,0582	485300	1703400	621710
Q5SSRQ6;P6787	Casein kinase II subunit beta CSNK2B;CSNK2B-tr	sp Q5SSRQ6 Q5SSRQ6_HUMAN Casein kinase II subunit beta OS=987590	8	26,925	2,0436	2,4349	1,2233	2,0436	5899500	15187000	987590
P08238;Q58FF	Heat shock protein HSP 90-beta HSP90AB1	sp P08238 HSP90B_HUMAN Heat shock protein HSP 90-beta OS=15600000	64	83,263	1,9891	2,9312	2,02	2,02	7615400	29148000	15600000
O95425;AOAJ!	Supervillin SVIL	sp O95425 SVIL_HUMAN Supervillin OS=Homo sapiens OX=213390	9	247,74	1,4281	3,0818	2,0134	2,0134	360680	1636100	213390
Q14676;A2AB0	Mediator of DNA damage checkpoint protein MDC1	sp Q14676 MDC1_HUMAN Mediator of DNA damage checkpoint protein MDC1	20	226,66	2,1653	2,0075	1,5305	2,0075	303620	152960	60101
Q14008;HOYDX	Cytoskeleton-associated protein 5 CKAP5	sp Q14008 CKAP5_HUMAN Cytoskeleton-associated protein 5	72	225,49	1,7242	2,0021	2,3599	2,0021	325010	2252600	1461800